Using the California Waterfowl Tracker to Assess Proximity of Waterfowl to Commercial Poultry in the Central Valley of California

Authors: Acosta, Sarai, Kelman, Todd, Feirer, Shane, Matchett, Elliott, Smolinsky, Jaclyn, et al.

Source: Avian Diseases, 65(3) : 483-492

Published By: American Association of Avian Pathologists

URL: https://doi.org/10.1637/aviandiseases-D-20-00137

AVIAN DISEASES 65:483–492, 2021

Regular Article—

Using the California Waterfowl Tracker to Assess Proximity of Waterfowl to Commercial Poultry in the Central Valley of California

Sarai Acosta,[A] Todd Kelman,[A] Shane Feirer,[B] Elliott Matchett,[C] Jaclyn Smolinsky,[D] Maurice Pitesky,[AE] and Jeffrey Buler[DE]

[A]Department of Population Health and Reproduction, School of Veterinary Medicine, VM3B #4007, University of California, Davis, 1 Shields Avenue, Davis, CA 95616
[B]Hopland Research and Extension Center, UC–Agriculture and Natural Resources, Hopland, CA 95449
[C]Dixon Field Station, Western Ecological Research Center, U.S. Geological Survey, Dixon, CA 95620
[D]Department of Entomology and Wildlife Ecology, University of Delaware, Newark, DE 19716

Received 28 June 2021; Accepted 2 July 2021; Published ahead of print 13 September 2021

SUMMARY. Migratory waterfowl are the primary reservoir of avian influenza viruses (AIV), which can be spread to commercial poultry. Surveillance efforts that track the location and abundance of wild waterfowl and link those data to inform assessments of risk and sampling for AIV currently do not exist. To assist surveillance and minimize poultry exposure to AIV, here we explored the utility of Remotely Sensed Moderate Resolution Imaging Spectroradiometer (MODIS) satellite imagery in combination with land-based climate measurements (e.g., temperature and precipitation) to predict waterfowl location and abundance in near real-time in the California Central Valley (CCV), where both wild waterfowl and domestic poultry are densely located. Specifically, remotely collected MODIS and climate data were integrated into a previously developed boosted regression tree (BRT) model to predict and visualize waterfowl distributions across the CCV. Daily model-based predictions are publicly available during the winter as part of the dynamic California Waterfowl Tracker (CWT) web app hosted on the University of California's Cooperative Extension webpage. In this study, we analyzed 52 days of model predictions and produced daily spatiotemporal maps of waterfowl concentrations near the 605 commercial poultry farms in the CCV during January and February of 2019. Exposure of each poultry farm to waterfowl during each day was classified as high, medium, low, or none, depending on the density of waterfowl within 4 km of a farm. Results indicated that farms were at substantially greater risk of exposure in January, when CCV waterfowl populations peak, than in February. For example, during January, 33% (199/605) of the farms were exposed for $\geq$1 day to high waterfowl density *vs.* 19% (115/605) of the farms in February. In addition to demonstrating the overall variability of waterfowl location and density, these data demonstrate how remote sensing can be used to better triage AIV surveillance and biosecurity efforts via the utilization of a functional web app–based tool. The ability to leverage remote sensing is an integral advancement toward improving AIV surveillance in waterfowl in close proximity to commercial poultry. Expansion of these types of remote sensing methods, linked to a user-friendly web tool, could be further developed across the continental United States. The BRT model incorporated into the CWT reflects a first attempt to give an accurate representation of waterfowl distribution and density relative to commercial poultry.

RESUMEN. Las aves acuáticas migratorias son el principal reservorio de los virus de la influenza aviar (con las siglas en inglés AIV), que pueden transmitirse a la avicultura comercial. Actualmente no existen esfuerzos de vigilancia que rastrean la ubicación y densidad de poblaciones de aves acuáticas silvestres y que vinculen esos datos para informar evaluaciones de riesgo y muestreo para influenza aviar. Para ayudar a la vigilancia y minimizar la exposición de la avicultura comercial a influenza aviar se exploró la utilidad de las imágenes satelitales por espectrorradiómetro de imágenes con resolución moderada (con las siglas en inglés MODIS) y de detección remota en combinación con mediciones climáticas terrestres (por ejemplo, temperatura y precipitación) para predecir la ubicación y densidad de aves acuáticas prácticamente en tiempo real en el Valle Central de California (CCV), donde tanto las aves acuáticas silvestres como las aves domésticas están densamente ubicadas. Específicamente, los datos MODIS y climáticos recopilados de forma remota se integraron en un modelo de árbol de regresión reforzado (BRT) desarrollado previamente para predecir y visualizar la distribución de las aves acuáticas en el Valle Central de California. Las predicciones diarias basadas en modelos están disponibles públicamente durante el invierno como parte de la aplicación dinámica en el del rastreador de aves acuáticas de California (California Waterfowl Tracker, CWT) ubicada en la página de internet de Extensión Cooperativa de la Universidad de California. En este estudio, se analizaron 52 días de predicciones del modelo y se produjeron mapas espacio-temporales diarios con densidades de aves acuáticas cerca de las 605 granjas avícolas comerciales en el Valle Central de California durante enero y febrero de 2019. La exposición de cada granja avícola a las aves acuáticas durante cada día se clasificó como alta, media, baja o nula, dependiendo de la densidad de aves acuáticas dentro de los cuatro kilómetros de una granja. Los resultados indicaron que las granjas tenían un riesgo sustancialmente mayor de exposición en enero, cuando las poblaciones de aves acuáticas en el Valle Central de California alcanzan su punto máximo, en comparación con febrero. Por ejemplo, durante enero, el 33% (199/605) de las granjas estuvieron expuestas durante más de un día a una alta densidad de aves acuáticas frente a un 19% (115/605) de las granjas en febrero. Además de demostrar la variabilidad general de la ubicación y densidad de las aves acuáticas, estos datos demuestran cómo se puede utilizar la teledetección para clasificar mejor los esfuerzos de bioseguridad y vigilancia para la influenza aviar mediante la utilización de una herramienta funcional basada en una aplicación en el internet. La capacidad de aprovechar la teledetección es un avance integral hacia la mejora de la vigilancia para influenza aviar en aves acuáticas en las proximidades de la avicultura comercial. La expansión de estos tipos de métodos de teledetección, vinculados a una herramienta en el internet que es fácil de usar, podría desarrollarse aún más en los Estados Unidos continentales. El modelo de árbol de regresión

[E]Corresponding authors. E-mail: mepitesky@ucdavis.edu; jbuler@udel.edu

reforzado incorporado en el sistema de rastreo de aves acuáticas de California refleja un primer intento de brindar una representación precisa de la distribución y densidad de las aves acuáticas en relación con las aves comerciales.

Key words: avian influenza, geospatial data, moderate resolution imaging spectroradiometer, poultry, remote sensing, waterfowl

Abbreviations: AIV = avian influenza virus; BRT = boosted regression tree; CSV = comma-separated values; HPAI = highly pathogenic avian influenza; MODIS = Moderate Resolution Imaging Spectroradiometer; CCV = California Central Valley; CWT = California Waterfowl Tracker; EO = Earth observations; NASS = National Agriculture Statistics Service; NFC = National Flyway Council; NWRS = National Wildlife Refuge System; NEXRAD = next generation radar; NPIP = National Poultry Improvement Plan; PRISM = Parameter-elevation Relationships on Independent Slopes Model; USDA = United States Department of Agriculture; USFWS = U.S. Fish and Wildlife Service; USGS = U.S. Geological Survey

Waterfowl migrate thousands of miles between wintering and breeding locations and have long been accepted as the natural reservoirs for LP (low pathogenic) and HP (highly pathogenic) avian influenza viruses (AIVs) (1,2,3,4,5,6,7). Both LP and HP AIVs can have a significant effect on commercial poultry morbidity and mortality. For example, the 2015 highly pathogenic avian influenza (HPAI) outbreak in North America represented the largest domestic animal disease outbreak in United States history, resulting in the loss of 48 million birds due to illness and culling and over US$3 billion in industry loss and federal expenditures to cover depopulation efforts (1).

Current national surveillance of AIV in commercial and backyard poultry is extensive temporally and spatially as part of the National Poultry Improvement Plan (NPIP) (2), and diagnostic laboratories in various states have passive AIV surveillance testing approaches. However, the waterfowl source population remains relatively under-surveilled. Specifically, in 2018 the U.S. Department of Agriculture (USDA) discontinued hunter-killed check station–based surveillance for AIVs in the continental United States. This change significantly reduced the ability to monitor AIV presence and subtype during the fall and winter, as outlined in the 2015 U.S. Interagency Strategic Plan led by the U.S. Geological Survey (USGS), U.S. Department of Food and Agriculture (USDA), U.S. Fish and Wildlife Service (USFWS), National Wildlife Refuge System (NWRS), and the National Flyway Council (NFC) (3).

Millions of waterfowl (about 60% of waterfowl in the Pacific Flyway and 18% continentally) use the CCV as a wintering location (4,5) because of climate, abundant habitat, and food resources (Fig. 1). Prevalence estimates have shown that between 5%–20% of migrating waterfowl in California shed AIV (6). The presence of waterfowl and their wetland habitats near poultry are suspected to increase AIV transmission risk in the United States and globally (7). Therefore, AIV risk analysis and preventative planning that accounts for spatiotemporal risk factors have been identified as a high priority in protecting poultry across the United States (8,9,10).

Frequent and high-resolution geospatial data predicting waterfowl location and abundance would enhance assessment and management of AIV transmission risk to commercial poultry operations. Although various remote sensing and land-based geospatial data exist and are open source, their application for managing exposure to waterfowl is nascent. Examples of datasets include Moderate Resolution Imaging Spectroradiometer (MODIS) and Landsat Thematic Mapper satellite imagery, used to detect surface moisture and land cover composition (i.e., habitat), and the Parameter-elevation Relationships on Independent Slopes Model (PRISM) Climate Group's land-based temperature and precipitation data (11,12). We previously used these datasets as spatially explicit predictors in a boosted regression tree (BRT) model (described in Materials and Methods) to better understand the presence-absence and density of waterfowl in the CCV during the high waterfowl density months of November to March as the basis for the California Waterfowl Tracker tool (13).

In this study, we explore a framework for using high-resolution and frequently updated spatially explicit data to help assess potential risk of poultry exposure to AIV via proximity to waterfowl in the CCV. Specifically, we analyzed the spatiotemporal relationship of potential exposure risk with 605 commercial poultry farms in the CCV over a 52-day period during January and February of 2019.

MATERIALS AND METHODS

Location data for poultry farms. In our analysis, we obtained 605 geocoded addresses of commercial poultry farms across the CCV from a state agency. For privacy purposes, point data were transformed into aggregate data at the county level, with the choropleth function via ArcGIS Pro (14) using government maps at the county level (Figs. 2, 3). The CCV is the major poultry production area in California and spatially overlaps with the majority of migratory and nonmigratory waterfowl in the California portion of the Pacific Flyway. Hence, the potential exposure of AIV from waterfowl to domestic commercial poultry is relatively high.

California Waterfowl Tracker. The CWT (13) is an interactive web-based mapping tool that provides near real-time raster maps, at 250-m spatial resolution, of predicted waterfowl density within the CCV. The CWT leverages a suite of 25 BRT models trained on archived weather-surveillance radar (i.e., NEXt generation RADar [NEXRAD]; National Weather Service) observations of waterfowl for the winters (November through February) of 2008–2017 from three NEXRAD stations, KDAX (Sacramento, CA), KBBX (Beale Air Force Base, CA), and KHNX (Fresno, CA) (15). The BRT models were trained from radar data of daily waterfowl densities aloft sampled at the instantaneous peak of evening feeding flight exodus (i.e., near the end of civil twilight) as birds departed diurnal roosting habitats following Buler *et al.* (15). Waterfowl densities are measured as the total, cross-sectional reflective area of birds in the airspace over the ground in units of cm^2/ha at a 250 × 250-m spatial resolution within radar domains. We partitioned the observed radar data into 25 subset groups of grid cells separated by 5 km distance on which to run the 25 modeling iterations to reduce spatial autocorrelation and allow assessing uncertainty across model predictions. The BRT models explained a mean of 53% of the variance in waterfowl density via cross-validation. The BRTs predict mean waterfowl density for each target day using environmental data from a 30-day window prior to the target day for each 250-m grid cell within the CCV. We provide maps of the daily predictions averaged across the 25 models.

The seven environmental predictor variables of the BRT model are (in order of descending relative importance): soil wetness index, total precipitation for 30 days prior, mean maximum daily temperature, mean daily temperature, month of year, proportion of rice cover flooded during the prior 30 days, and proportion of permanent wetland cover. We estimated soil wetness using the MODIS reflectance data product

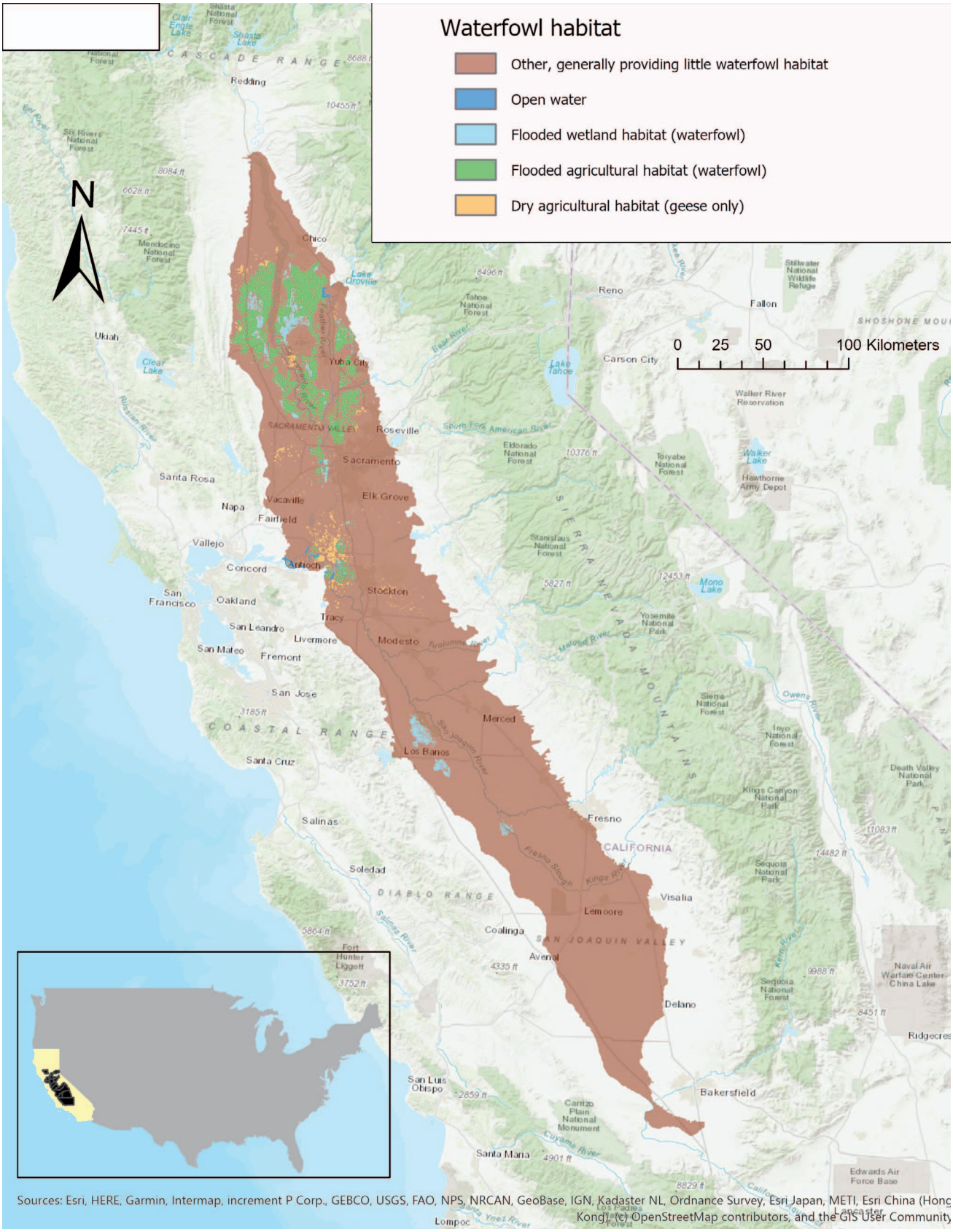

Fig. 1. This map identifies waterfowl habitat distributions in the CCV using various data including soil wetness and surface water flooding. Primary waterfowl habitats, including dry corn fields, flooded rice and corn fields, and flooded wetlands in the CCV, are used by waterfowl during the winter. Other, less-frequently used land cover includes lakes, other cropland, and urban landscapes. Flooded rice fields are predicted to receive the greatest intensity of use for roosting by waterfowl. Dry agricultural fields (e.g., rice and corn) provide habitat for feeding. The map was derived using cropland and open water land cover data from Cropscape (USDA) (18), wetlands land cover data from the Central Valley Joint Venture (28), and tasseled cap transformed MODIS data (16).

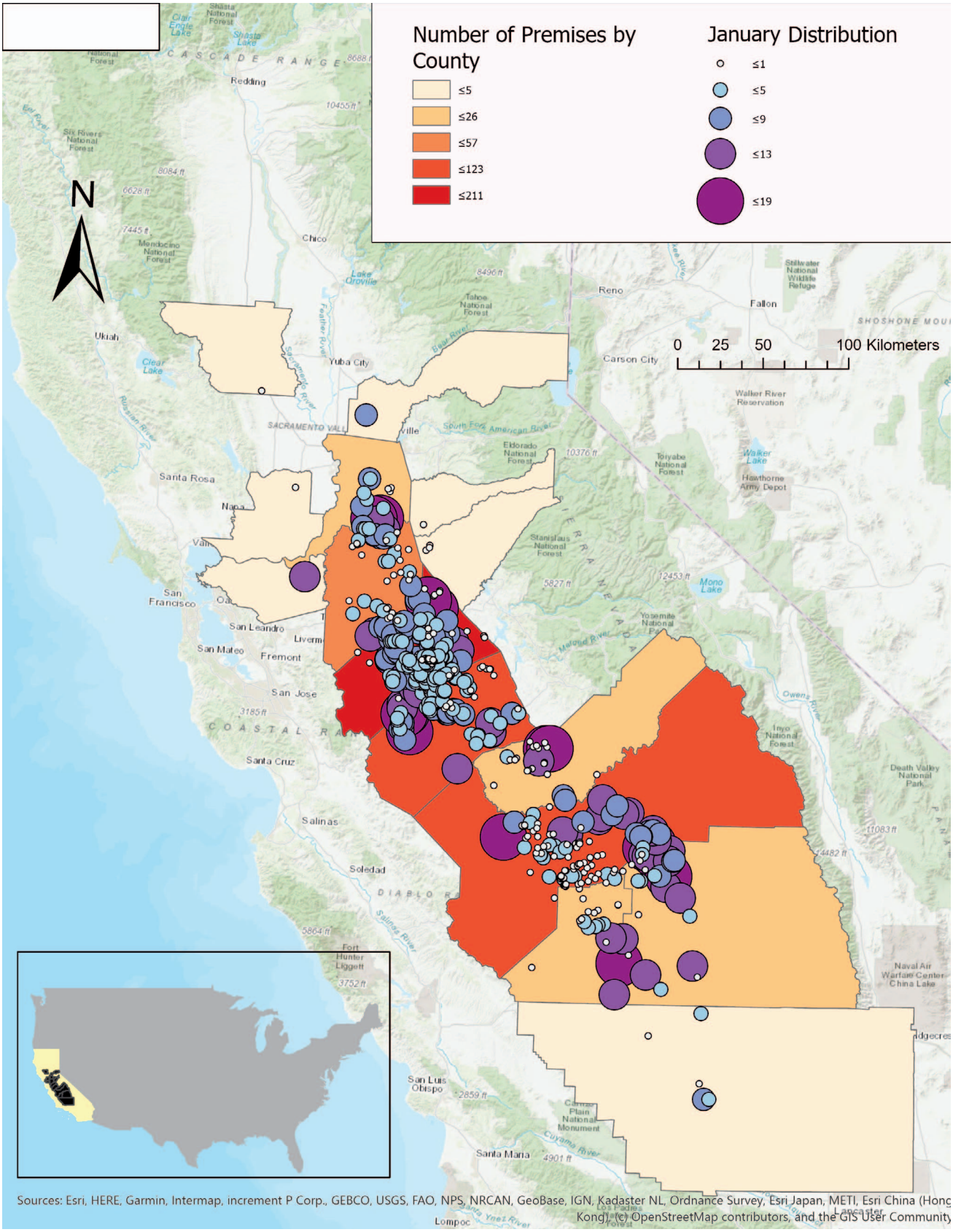

Fig. 2. Choropleth map of commercial poultry farms by county in the CCV overlayed with proportional symbology representing the number of occurrences any given farm was included in a high-density waterfowl area during January of 2019.

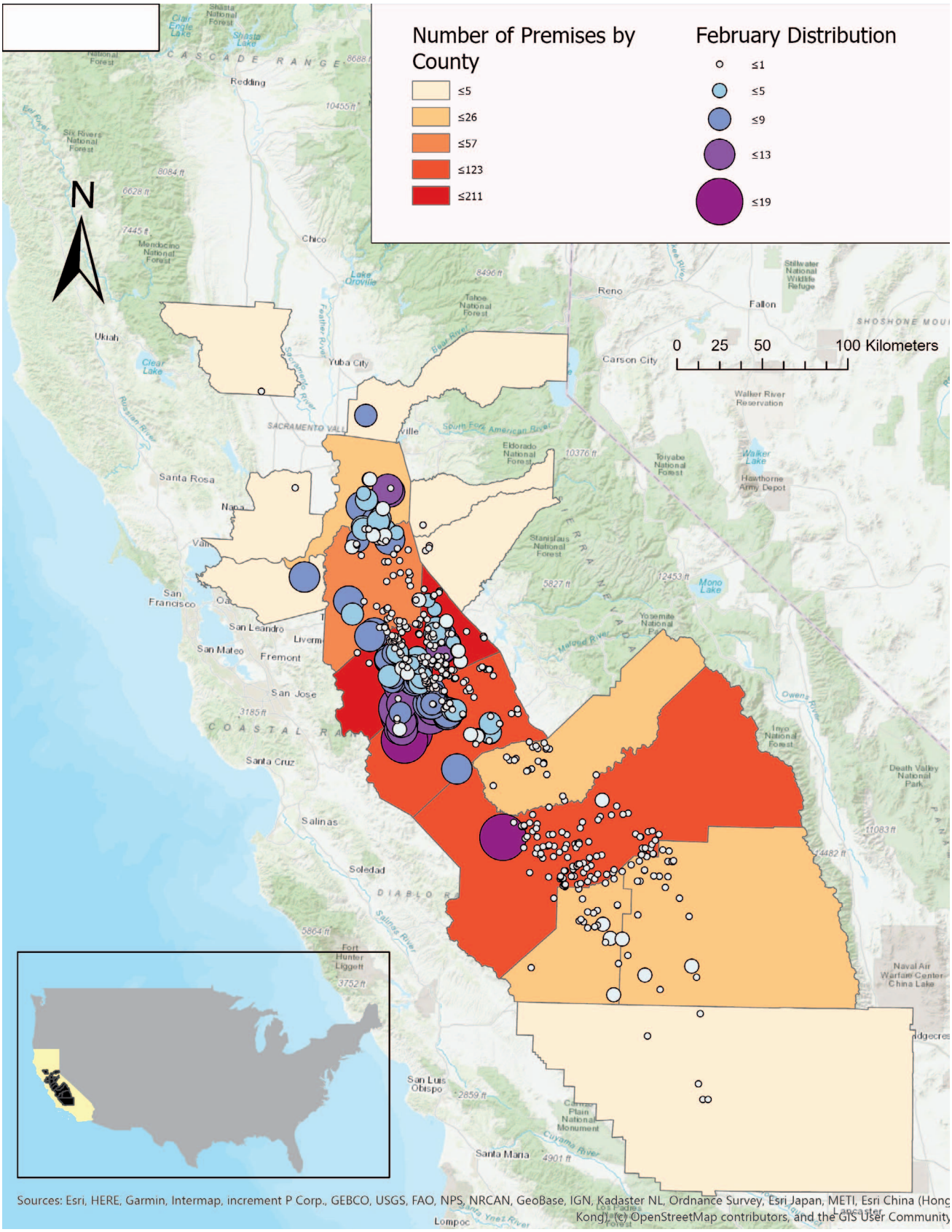

Fig. 3. Choropleth map of commercial poultry farms by county in the CCV overlayed with proportional symbology representing the number of occurrences any given farm was included in a high-density waterfowl area during February of 2019.

Table 1. Percentage of farms and duration (days) that corresponded with high, medium, low, and none densities of waterfowl in the CCV during January and February of 2019. Farm locations were intersected with spatially explicit waterfowl distributions predicted daily with a BRT model.

Metrics of farm-waterfowl correspondence	Waterfowl density categories	January–February study period	January	February
Mean percent of time in days of farm in each density category	High	3	3	3
	Medium	13	21	6
	Low	15	18	13
	None	69	65	78
Percent of farms spending at least 1 day in each density category	High	41	33	19
	Medium	82	83	42
	Low	98	94	73
	None	100	99	100

MCD43A4 V006 (Nadir BRDF-Adjusted Reflectance) obtained from the USGS's Land Processes Distributed Active Archive Center (LPDAAC). The MCD43A4 V006 contains seven reflectance bands averaged over a 16-day window at 500-m resolution. We used tasseled cap transformations for MODIS data as described by Lobser and Cohen (16) via the Tasseled Cap function from the R package MODIS (17) to derive wetness indices. We obtained total precipitation and mean and maximum temperature for each of 30 days prior to prediction day from the PRISM Climate Group (11,13). For characterizing the proportion of rice and wetland composition within grid cells, we used the geospatial Cropland Data Layer (year 2019) from the USDA and National Agriculture Statistics Service (NASS) (18). Flooded rice fields are often easy to delineate from aerial photos because the field boundaries are rather discrete. Therefore, following Sieges *et al.* 2014 (19), we visually inspected the MODIS soil wetness imagery overlaid with NASS crop maps and aerial images of open surface-water conditions (flooded soil) to determine that areas having index values greater than −0.125 were flooded.

Through the online interface, users can upload a delimited, comma-separated values (CSV) file containing geocoded areas of interest. A built-in data processing feature allows for the locations to be paired with mean predicted waterfowl density estimates within 4 km of each of the given geocoded locations for the previous 28 days. In this fashion we used the CWT to assess daily variability in nearby 2 waterfowl densities for the 605 farms in the CCV for the study period of January–February 2019.

Data processing. We generated predicted daily waterfowl density raster maps for the CCV between January and February of 2019 for the CWT. We processed map data with ArcGIS Pro (14) and computed diagnostic frequency-based statistics (14,20). Predicted waterfowl density data within each grid cell was first classified into 4 classes: none ($<$1.0 cm^2/ha), low (1.0 – 2.5 cm^2/ha), medium (2.5 – 15.0 cm^2/ha), and high ($>$15.0 cm^2/ha). We determined these classes by dividing the distribution of values above a minimum threshold of 1 cm^2/ha for reflectivity of waterfowl exodus into three approximately equal quantiles. We used this minimum threshold based on visually matching the footprint of reflectivity to the boundary of known wetland areas used by waterfowl. Next, the categories of predicted waterfowl density (i.e., potential risk of waterfowl exposure) within a 4-km radius window around each grid cell were calculated using the average feeding flight distance of waterfowl in the CCV (21). The CWT interfaces with ArcGIS to extract and store the most recent 28 days of PRISM and MODIS data to use in BRTs for modeling waterfowl densities. Using geocoded locations on a CSV file, data were recorded for 52 total days, for each day at each specific geocoded location.

We derived the statistics in Table 1 by compiling the frequencies of each occurrence of high, medium, low, and none for each of the 605 farms (22,23). Percentages were calculated based on the average mean equation

$$\left(\frac{\sum \text{of occurrences per farm}}{\text{number of days} \in \text{the study}(52\text{ days})}\right) \times 100,$$

where one occurrence = 1 day in a category and farm = farm boundary for each of the given categories. We compiled Figures 2 and 3 with ArcGis Pro by overlaying the frequency of high occurrences for each farm.

RESULTS

Data management. Due to server errors, we could not predict seven of the intended 59 days and these data were not recorded. Omitted dates include Jan. 1,18,19,20 (4/30 days) as well as February 5,6,28 (3/28 days).

Temporal variation in waterfowl densities near poultry. Spatially explicit waterfowl density varied substantially among poultry farms (Table 1; Figs. 2, 3), geography-climatic conditions (Figs. 4, 5), and day (Fig. 6). Density and distribution of waterfowl near commercial poultry farms changed as a function of time (Table 1) and climatic conditions according to BRT predictive modeling. Reflecting this variability during the study period, 41% (248 farms) of the 605 farms spent at least one day in a 'high' waterfowl density area and 98% (593 farms) spent at least one day in 'low,' and 100% (605 farms) spent at least one day in the 'none' waterfowl density area.

While none of the 605 farms spent the entire study period of 52 days in one of the high, medium, or low categories, 2% (11 farms) of the 605 farms spent the entire study period in the none category. The maximum days a facility spent in the high, low, and none categories were 43 days (83% of the study period), 20 days (39% of the study period), and 52 days (100% of the study period), respectively.

In January, although farms infrequently corresponded with locations of very high waterfowl density (3% of days on average), farms frequently corresponded with moderate to low waterfowl densities on approximately 40% of the days (Table 1). Even though farms infrequently corresponded with high densities of waterfowl, many farms (33%) were in relatively high (33%) to moderate risk (83%) areas on at least one day during January (Table 1). Relatively high densities for January were seen between the 23rd and 27th (Figs. 4, 6).

In February, the mean percentage of time that farms spent in the medium and low categories was lower than in January (Table 1). Likewise, the percentage of farms that spent at least one day in the high, medium, or low categories in February were lower than in January (Table 1). Relatively high densities for February were seen between the 12th and 17th when the frequency of high-density occurrences peaked, whereas frequency of high density was relatively

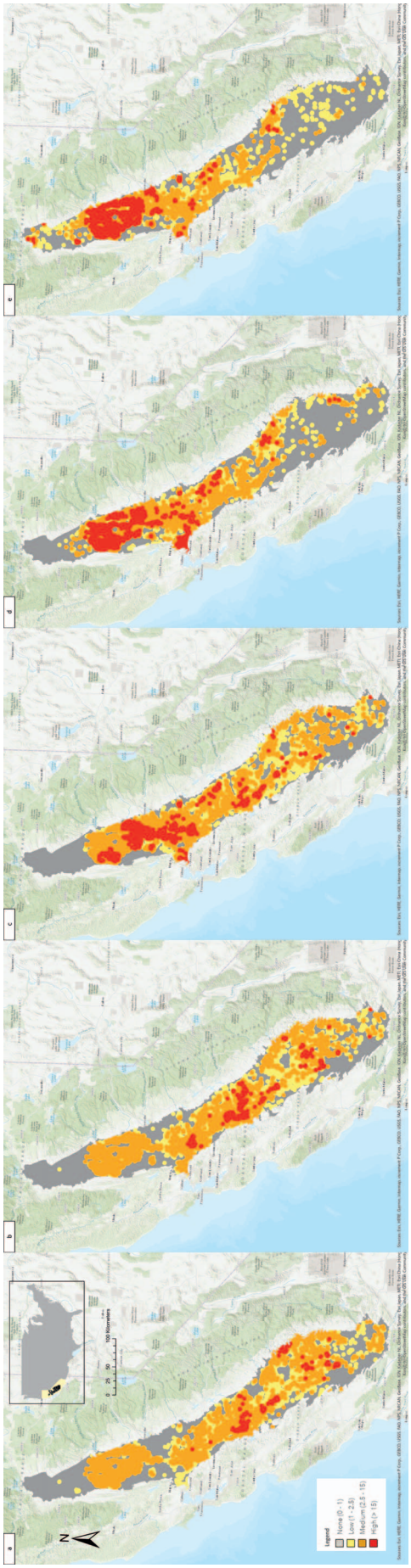

Fig. 4. (a–e) Predicted daily CWT waterfowl density between (a) January 22, and (e) January 26 of 2019. Colored circles represent the predicted density for high (red), medium (orange), low (yellow), and none (gray) waterfowl in the California Central Valley. Each circle represents a 4-km–diameter area.

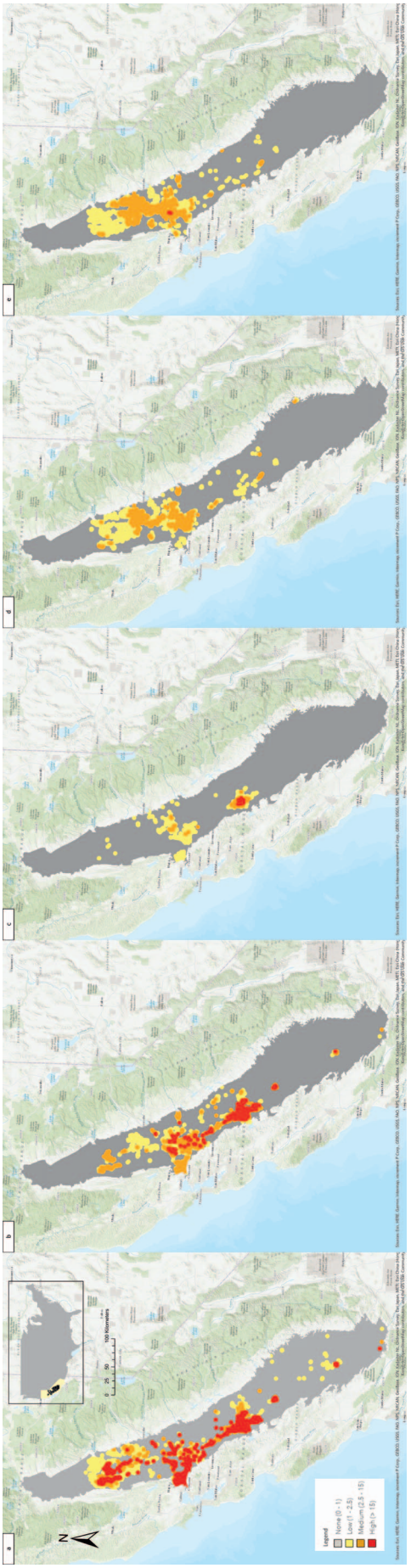

Fig. 5. (a–e) Predicted daily CWT waterfowl density between (a) February 13th, and (e) February 17th of 2019. Colored circles represent the predicted density for high (red), medium (orange), low (yellow), and none (gray) waterfowl in the CCV. Each circle represents a 4-km–diameter area.

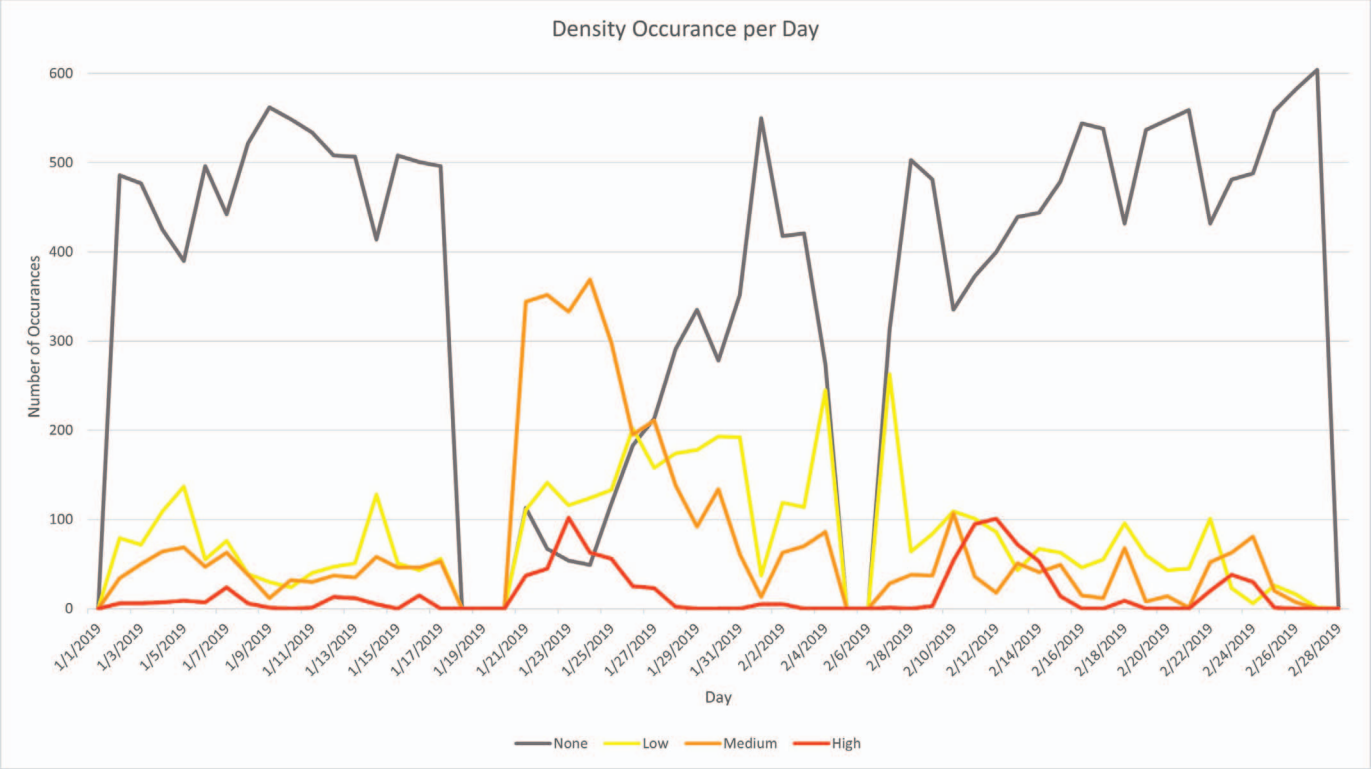

Fig. 6. Frequency of the 605 commercial farms in the high, medium, low, and none waterfowl density categories for each of the 52 days during January and February of 2019. The gaps represent the days with missing data.

low the rest of the month with a small peak again toward the end of the month between February 22 and 24 (Figs. 5, 6).

Figures 4a–e and 5a–e show the daily BRT-predicted waterfowl distribution provided by the CWT for January 23 and 27 and February 13 and 17; these reflect the highest overall density and distribution of waterfowl during the months of January and February, respectively (Fig. 6). The geographic variability of those waterfowl can be seen in Figures 4 and 5. The variability reflects changes in the seven environmental predictor variables of the BRT model.

Spatial variation in waterfowl density near poultry. For the entire study period, the northern and central parts of the CCV had the highest waterfowl activity (Figs. 4, 5). At the county level and with respect to poultry farms, central CCV farms within Stanislaus (211 farms), Fresno (123 farms), and Merced (108 farms) counties were near the highest density of waterfowl during January (Fig. 2). In contrast, waterfowl densities were generally lower near farms in southern CCV counties, such as Tulare (26 farms) and Madera (24 farms; Fig. 2). Although waterfowl density was relatively lower near farms in February, some farms in Stanislaus and Merced counties had some of the highest densities of waterfowl in February seen during the entire study period.

DISCUSSION

From a biosecurity perspective, the overall spatiotemporal variability of waterfowl concentrations (Table 1, Figs. 2–6) as an index of AIV exposure risk to poultry farms demonstrates that the static surveillance approaches currently employed by the NPIP for commercial poultry, and the 2015 U.S. Interagency Strategic Plan for waterfowl, are not optimal. Results specifically indicated that farms differ markedly in their proximity to waterfowl across space and time during the winter months. Frequently updated dynamic maps of waterfowl distributions could be used to triage risk of exposure to AIV among poultry farms and allow a near real-time response to risk. The vast majority (82%) of farm locations corresponded with moderate or high waterfowl densities on at least 1 day, mostly during the last week of January (Fig. 6). Correspondence of high waterfowl densities with farms is relatively temporary (3% of days on average during January and February in 2019). However, 3 of the 4 days that lacked data in January (1/18–1/20) because of server errors occurred 3 days before the 1/23–1/27 moderate-high waterfowl density event, and so the number of moderate or high-density days may have been slightly underestimated.

From a biosecurity perspective, producers should consider the best way to utilize the CWT and the associated data during the relatively short time of peak risk. For example, organic producers, which in the United States are required to provide outdoor access to their flocks, could increase their biosecurity by keeping their birds indoors via an exemption from regulators.

During the study period, the predicted waterfowl density near poultry farms was greater in January than in February, with the waterfowl distribution and density localized in the northern CCV. This observation makes sense from a waterfowl habitat perspective, as demonstrated by Figure 1, which identifies waterfowl habitat distributions in California. Of the seven predictive variables integrated into the BRT predictive model, the soil wetness index was identified as the most important variable in predicting waterfowl use. Specifically, the majority of the waterfowl habitat in the CCV is in the northern and central parts of the CCV (Fig. 1). However, it is

also important to recognize that Figure 1 primarily reflects permanent and semipermanent habitat. Conditions such as seasonal rains can create temporarily flooded habitat for waterfowl. Static waterfowl habitat maps do not capture this habitat variability in contrast to the BRT predictive waterfowl maps in Figures 4 and 5, which show daily geographic changes in waterfowl distribution and density. Hence, the ability to make daily predictions is a critical function of the CWT and for the assessment of relative AIV exposure risk to commercial poultry.

While infectious agents like AIVs transmitted between wildlife and commercial poultry are considered a threat to poultry production and food security globally, current surveillance and risk analysis efforts are limited. The use of remote sensing technologies, including satellite imagery and land-based surface sensors, in food animal agriculture is relatively nascent in contrast with its use for crop-based agriculture (24,25). The BRT model incorporated into the CWT reflects a first attempt to give an accurate representation of waterfowl distribution and density relative to commercial poultry. We anticipate future use of the CWT to help triage AIV testing as opposed to the swabbing of waterfowl based on a static surveillance model developed as part of the 2015 U.S. Interagency Strategic Plan (3). The "needle in the haystack" and convenience-based static surveillance are costly, time consuming, and epidemiologically unsound. The application of validated statistical models that use updated predictor variables to create spatiotemporally explicit models is one potential method toward the development of a robust risk-based model. Even then, the output must be available in a unifying and user-friendly format, such as the CWT, in order to enable stakeholder understanding of the risk landscape.In its current form, the CWT only predicts waterfowl distributions and densities in near real-time between November and March, which represents the period when waterfowl in the Pacific Flyway winter in the CCV. While the CWT does not identify the species, age, or presence-absence of AI in waterfowl, it provides important information that could be used by farmers and other stakeholders to triage husbandry and biosecurity efforts relative to the presence and density of waterfowl. In addition, while the presence of these habitats may support waterfowl now, the removal of these habitats that resulted from climate change, water management, or conversion to other land uses, or the addition of habitat resulting from conservation programs, will likely affect distribution, density, and proximity to commercial poultry in the CCV. To that point, the CWT could be an invaluable tool toward understanding how these changes affect the spatiotemporal relationship between commercial poultry and waterfowl. The collection of multiple years of data will be critical toward understanding potential trends in waterfowl movements.

It is also important to recognize that the BRT model does not integrate other risk factors including husbandry, biosecurity practices, AIVs persistence in the environment, and other avian bridge hosts that may be carriers of AIVs. While proper biosecurity is not a novel technology, it is a fundamental aspect of flock management and disease prevention. Using the CWT could be an additional tool used by producers and stakeholders to better assess risk and complement husbandry and biosecurity practices. For example, a producer could use this information to better select future operations and husbandry types. Additionally the CWT could be used to facilitate targeted sampling of the environment for AIVs to better understand environment as a risk factor (26).

Despite CWT capabilities, its prediction of waterfowl density and distribution and risk assessment for poultry farms could be improved and requires additional evaluation. Future efforts can improve modeling of waterfowl distributions within the CCV. For example, while the BRT model used was constructed using historical radar observations from 2008–2017, automated processing of radar data in near real-time would allow continuous training and updating of the BRT model to improve model predictions. Additionally, USGS scientists have developed extensive telemetry datasets (year 2015–ongoing) that track locations of individual waterfowl in the CCV and across the Pacific Flyway. These telemetry data include approximately 890 ducks of 10 species and 240 geese of four species-subspecies, and $>$8 million point locations (Matchett, pers. comm.). The advanced telemetry used provides very high-resolution ($<$10 m) accuracy and frequent location data of tagged waterfowl (22,26). Both radar and telemetry data streams are in the process of being integrated into the CWT to provide further insights about waterfowl distributions throughout the day and year.

With respect to risk analysis, our results indicate that AI risk analysis and preventative planning that accounts for local waterfowl activity is a high priority for the protection of poultry across the United States. The application of this approach across the United States could include the utilization of climatologically aided interpolation of the over 10,000 PRISM surface stations across the United States (6). With respect to Earth observations (EO), the number of EO-based satellites is increasing at an astonishing pace, from 192 in 2014 to 684 EO-based satellites in 2018 (23). In addition, as these satellites move from a geo-polar orbit to a geo-stationary orbit, continuous imaging of the entire earth becomes a more realistic option. Particularly interesting is the adoption of cubesats (i.e., small boxy satellites weighing a few kilograms each) for which, due to their small size, dozens can be put into orbit during a single launch, thereby reducing cost and making custom collection of data for different projects viable. These networked satellites facilitate the imagery of the entire Earth's surface multiple times/day (27).

Lacking the ability to understand the dynamic spatiotemporal relationship between poultry farms and their proximity to waterfowl and waterfowl habitat, producers and stakeholders have few options other than biosecurity and NPIP-based surveillance. Although remote sensing of waterfowl does not provide a comprehensive risk analysis with respect to AIV, the use of remote sensing tools are highly understudied in AIV risk analyses. The ability to use remote sensing to guide AI sampling in waterfowl has previously been demonstrated (26). The application of approaches that integrate risk-based surveillance with models that utilize various modes of EO will likely play a role in AIV surveillance over the coming decades in the poultry industry.

REFERENCES

1. Greene JL. *Update on the highly-pathogenic avian influenza outbreak of 2014–2015*. Washington DC: Congressional Research Service. Report R44114. 2015.

2. U.S. Department of Agriculture, Animal and Plant Health Inspection Service [USDA, APHIS]. *National poultry improvement plan*. Washington DC: USDA, APHIS [modified 2020 Jun 2; accessed 2021 Jun 26]. https://www.aphis.usda.gov/aphis/ourfocus/animalhealth/nvap/NVAP-Reference-Guide/Poultry/National-Poultry-Improvement-Plan.

3. U.S. Geological Survey, U.S. Department of Food and Agriculture, U.S. Fish and Wildlife Service, National Wildlife Refuge System, and the National Flyway Council. *Early detection and monitoring for avian influenzas of significance in wild birds: a U.S. interagency strategic plan*. Washington DC: USGS, USDA, USFWS, NWRS, NFC. 2015. https://www.aphis.usda.gov/

animal_health/downloads/animal_diseases/ai/wild-bird-strategic-plan.pdf; 2015.

4. Ramey AM, Hill NJ, Cline T, Plancarte M, De La Cruz S, Casazza ML, Ackerman JT, Fleskes JP, Vickers TW, Reeves AB. Surveillance for highly pathogenic influenza A viruses in California during 2014–2015 provides insights into viral evolutionary pathways and the spatiotemporal extent of viruses in the Pacific Americas Flyway: influenza A viruses in California during 2014–2015. *Emerg Microbes Infect*. 6:1–10; 2017.

5. Gilmer DS, Miller MR, Bauer RD, LeDonne JR. California's Central Valley wintering waterfowl: concerns and challenges. In: Sabol K, editor. *Transactions of the forty-seventh north american wildlife and natural resources conference*. 1982 March 26–31; Portland, (OR): *US Fish & Wildlife Publications*. p. 441–452; 1982.

6. Henaux V, Samuel MD, Dusek RJ, Fleskes JP, Ip HS. Presence of avian influenza viruses in waterfowl and wetlands during summer 2010 in California: are resident birds a potential reservoir? *PLOS ONE* 7:e31471; 2012. doi.org/10.1371/journal.pone.0031471.

7. Olsen B, Munster VJ, Wallensten A, Waldenström J, Osterhaus AD, Fouchier RA. Global patterns of influenza A virus in wild birds. *Science* 312:384–388; 2006.

8. Fang L-Q, de Vlas SJ, Liang S, Looman CW, Gong P, Xu B, Yan L, Yang H, Richardus JH, Cao W-C. Environmental factors contributing to the spread of H5N1 avian influenza in mainland China. *PLOS ONE* 3:e2268; 2008. doi.org/10.1371/journal.pone.0002268.

9. Flint PL, Pearce JM, Franson JC, Derksen DV. Wild bird surveillance for highly pathogenic avian influenza H5 in North America. *Virology J*. 12:1–6; 2015.

10. Si Y, de Boer WF, Gong P. Different environmental drivers of highly pathogenic avian influenza H5N1 outbreaks in poultry and wild birds. *PLOS ONE* 8:e53362; 2013. doi.org/10.1371/journal.pone.0053362

11. Daly C. *Descriptions of PRISM spatial climate datasets for the conterminous United States*. Corvalis, (OR): Northwest Alliance for Computational Science & Engineering; 2013.

12. Torbick N, Salas WA, Hagen S, Xiao X. Monitoring rice agriculture in the Sacramento Valley, USA with multitemporal PALSAR and MODIS imagery. *IEEE J Sel Top Appl Earth Obs Remote Sens*. 4:451–457; 2010.

13. Feirer S, Kelamn T, Pitesky M, Buler J. California Waterfowl Tracker (CWT). [Internet]. 2017 [cited 2021 June 6]. Available from: https://www.arcgis.com/apps/webappviewer/index.html?id=859cc2b3d28d4372865afa2ba2457a2d

14. ESRI. ArcGis Pro, version 2.4. Redlands (CA): ESRI. https://www.esri.com/en-us/arcgis/products/arcgis-pro/overview; 2019.

15. Buler JJ, Randall LA, Fleskes JP, Barrow Jr WC, Bogart T, Kluver D. Mapping wintering waterfowl distributions using weather surveillance radar. *PLOS ONE*. 7:e41571; 2012. doi.org/10.1371/journal.pone.0041571

16. Lobser S, Cohen W. MODIS Tasselled Cap: land cover characteristics expressed through transformed MODIS data. *Int J Remote Sens*. 28:5079–5101; 2007.

17. Mattiuzzi M, Verbesselt J, Hengl T, Klisch A, Stevens F, Mosher S, Evans B, Lobo A, Detsch F. *MDF M. MODIS: Acquisition and Processing of MODIS Products,* version 1.2.3. Goldcoast, (Australia): RDRR. IO. https://rdrr.io/cran/MODIS/man/MODIS-package.html; 2019.

18. U.S. Department of Agriculture, National Agricultural Statistics Service [USDA, NASS]. *Cropland data layer*. Washington, DC: USDA, NASS, Marketing and Information Services Office [modified 2021 Jun 23; accessed 2021 Apr]. http//nassgeodata.gmu.edu/Crop-Scape; 2003.

19. Sieges ML, Smolinsky JA, Baldwin MJ, Barrow Jr WC, Randall LA, Buler JJ. Assessment of bird response to the migratory bird habitat initiative using weather-surveillance radar. *Southeast Nat*. 13:G36–G65; 2014.

20. R Core Team. RStudio: integrated development for R, version 3.6.2. Vienna (Austria): R Foundation for Statistical Computing. http://www.R-project.org; 2020.

21. Fleskes J, Yee J, Casazza ML, Miller M, Takekawa JY, Orthmeyer D. *Waterfowl distribution, movements, and habitat use relative to recent habitat changes in the Central Valley of California: a cooperative project to investigate impacts of the Central Valley Habitat Joint Venture and changing agricultural practices on the ecology of wintering waterfowl*. Dixon (CA): U.S. Geological Survey-Western Ecological Research Center; 2005.

22. McDuie F, Casazza ML, Keiter D, Overton CT, Herzog MP, Feldheim CL, Ackerman JT. Moving at the speed of flight: dabbling duck-movement rates and the relationship with electronic tracking interval. *Wildl Res*. 46:533–543; 2019.

23. Pixalytics. How many Earth observation satellites are in space in 2018? 2018; 1–3. Availabe from https://www.pixalytics.com/eo-satellites-in-space-2018.

24. Brewster CC, Allen JC, Kopp DD. IPM from space: using satellite imagery to construct regional crop maps for studying crop–insect interaction. *Am Entomol*. 45:105–117; 1999.

25. Lucas R, Rowlands A, Brown A, Keyworth S, Bunting P. Rule-based classification of multi-temporal satellite imagery for habitat and agricultural land cover mapping. *ISPRS Int J Geoinf*. 62:165–185; 2007.

26. McCuen MM, Pitesky ME, Buler JJ, Acosta S, Wilcox AH, Bond RF, Díaz-Muñoz SL. A comparison of amplification methods to detect avian influenza viruses in California wetlands targeted via remote sensing of waterfowl. *Transbound Emerg Dis*. 68:98–109; 2020.

27. Selva D, Krejci D. A survey and assessment of the capabilities of Cubesats for Earth observation. *Acta Astronautica* 74:50–68; 2012.

28. Petrik K, Fehringer D, Weverko A. *Mapping seasonal managed and semi-permanent wetlands in the Central Valley of California*. Rancho Cordova (CA): Ducks Unlimited. Ducks Unlimited Project US-CV-5-3. 2014.